PROFESSOR GUILLERMO SCHMEDA HIRSCHMANN (Orcid ID : 0000-0002-9228-5378)

Article type : Research Article

Inhibition of key enzymes in the inflammatory pathway by hybrid molecules of terpenes and synthetic drugs: *in vitro* and *in silico* studies

Running title: Anti-inflammatory effect of terpene-NSAIDs hybrids

Cristina Theoduloz[1,2], Jans Alzate-Morales[3], Felipe Jiménez-Aspee[2,4,5], Maria Inés Isla[6], María Rosa Alberto[6], Mariano Walter Pertino[2,7], Guillermo Schmeda-Hirschmann[2,7]

[1]Laboratorio de Cultivo Celular, Facultad de Ciencias de la Salud, Universidad de Talca, Talca 3460000, Chile.

[2]Programa de Investigación de Excelencia Interdisciplinaria en Química y Bio-orgánica de Recursos Naturales (PIEI-QUIM-BIO), Universidad de Talca, Talca 3460000, Chile.

[3]Centro de Bioinformática y Simulación Molecular (CBSM), Universidad de Talca, Talca 3460000, Chile.

[4]Departamento de Ciencias Básicas Biomédicas, Facultad de Ciencias de la Salud, Universidad de Talca, Talca 3460000, Chile.

[5]Núcleo Científico Multidisciplinario, Dirección de Investigación, Universidad de Talca, Talca 3460000, Chile.

[6]Laboratorio de Investigación de Productos Naturales (LIPRON), Instituto de Química del NOA (INQUINOA-CONICET). Facultad de Ciencias Naturales e IML. Universidad Nacional de Tucumán, San Miguel de Tucumán, Tucumán, Argentina.

[7]Laboratorio de Química de Productos Naturales, Instituto de Química de Recursos Naturales, Universidad de Talca, Talca 3460000, Chile.

This article has been accepted for publication and undergone full peer review but has not been through the copyediting, typesetting, pagination and proofreading process, which may lead to differences between this version and the Version of Record. Please cite this article as doi: 10.1111/cbdd.13415

Correspondence
Guillermo Schmeda-Hirschmann, Laboratorio de Química de Productos Naturales, Instituto de Química de Recursos Naturales, Universidad de Talca, Talca 3460000, Chile.
E-mail: schmeda@utalca.cl
Phone: +56-7122-00288

KEYWORDS
Ibuprofen and naproxen terpenyl hybrids, COX-2 and 15-LOX inhibition, anti-inflammatory activity, *in silico* studies, computational analysis

ABSTRACT

The aim of this work was to compare the anti-inflammatory activity of compounds prepared from terpenes and the synthetic drugs ibuprofen and naproxen. The anti-inflammatory activity of the hybrid compounds was compared with the activity of the parent compounds. This was accomplished using *in vitro* inhibition of LOX and COX-2, and *in silico* docking studies in 15-LOX and COX-2. The synthesized hybrids showed an inhibition of COX-2 and LOX between 9.8-57.4% and 0.0-97.7%, respectively. None of the hybrids showed an improvement in the inhibitory effect towards these pro-inflammatory enzymes, compared to the parent terpenes and NSAIDs. The docking studies allowed us to predict the potential binding modes of hybrids **6 - 15** within COX-2 and 15-LOX active sites. The relative affinity of the compounds inside the binding sites could be explained by forming non covalent interactions with most important and known amino acids reported for those enzymes. A good correlation (r^2 =0.745) between docking energies and inhibition percentages against COX-2 was found. The high inhibition obtained for compound **10** against COX-2 was explained by hydrogen bond interactions at the enzyme binding site. New synthetic possibilities could be obtained from our *in silico* models, improving the potency of these hybrid compounds.

1| INTRODUCTION

The cyclooxygenases are enzymes that catalyse the two initial steps in prostaglandin biosynthesis. Both isoforms of the enzyme, namely COX-1 and COX-2, are targets of non-steroidal anti-inflammatory drugs (NSAIDs) [1]. COX-1 is expressed constitutively in most cells, while COX-2 is up-regulated by cytokines, shear stress and growth factors. In this sense, COX-1 is considered to act in housekeeping functions, while COX-2 is the major source

of prostanoids formed in inflammation and cancer [2]. A third COX, COX-3, is a splice variant of COX-1 that retains enzymatic activity with no clear role up to this point [3].

NSAIDs are inhibitors of COX-2, thus exerting anti-inflammatory effects. The inhibition of COX-1 is associated with the undesirable side-effects of these drugs. Therefore, compounds with selective COX-2 inhibition are looked-for therapeutic agents [4]. As organic acids, these drugs have good bioavailability, have high binding percentages to plasma proteins and are accumulated in sites of inflammation. Among NSAIDs, ibuprofen is a widely commercialized anti-inflammatory drug with non-selective COX inhibitory effects. The structure of COX-2 bound to ibuprofen has been elucidated [5], offering new insights for *in silico* studies of COX inhibitors. Most NSAIDs are organic acids that act by competitive and reversible inhibition of COX, with the exception of Aspirin® which irreversible antagonizes the action of COX by acetylation of Ser530 in COX-1 and Ser516 in COX-2 [6].

Lipoxygenases (LOX) are a family of non-heme iron containing enzymes that catalyse the oxygenation of polyenic fatty acids (i.e. arachidonic acid) into the corresponding lipid hydroperoxide eicosatetraenoic acids (HPETEs). There are five human lipoxygenases, namely, 5-LOX, 12(S)-LOX, 12(R)-LOX, 15-LOX and 15-LOX-2, classified according to the site of hydroperoxy group insertion and stereoconfiguration [7]. Their expression is frequently cell specific, and among them, the 5-LOX pathway leads to the synthesis of leukotrienes (LTs), which play a major role in the development and persistence of the inflammatory response. The reduction and chelation of the non-heme iron present in the catalytic site of the enzyme is proposed as the mechanism of action of 5-LOX inhibitors, such as zileuton [9]. Dual inhibition of COX-2 and 5-LOX is also a therapeutic alternative to treat inflammation with a better safety profile [8,9].

The three-dimensional X-ray structure of the enzymes COX-2 and LOX has been described. These studies allowed *in silico* experiments in order to understand the intermolecular interactions of selected compounds within the binding or active site of these enzymes. For instance, the synthesis of Aspirin® analogues as dual COX-2/5-LOX inhibitors was reported [9]. This feature was achieved by incorporating a NO-releasing sulfohydroxamic group (SO_2NHOH) in the synthetic analogues of the pharmacophore. *In vitro* COX-1/COX-2 isozyme inhibition studies identified 2-hydroxysulfamoylbenzoic acid, 2-benzyloxysulfamoylbenzoic acid and 2-hydroxysulfamoylbenzoic acid ethyl ester as highly

potent and selective COX-2 inhibitors [10]. Moreover, 2-hydroxysulfamoylbenzoic acid and 2-hydroxysulfamoylbenzoic acid ethyl ester, with the sulfohydroxamic acid moiety, showed potent 5-LOX inhibitory activity. Molecular docking studies in the active binding site of COX-2 and 5-LOX provided complementary theoretical support for the experimental biological structure-activity data acquired. The synthesis, dual COX/LOX inhibition, molecular modeling and cytotoxicity of a series of di-tertiary-butyl phenylhydrazones was reported [10]. Molecular docking studies revealed a good fit of these compounds in the COX-2 and 5-LOX protein cavities.

The design of hybrid compounds including synthetic moieties and NSAIDs has been explored, including the hybrids of Aspirin® [11], and new compounds including terpene moieties [12]. We have previously reported the *in vivo* anti-inflammatory effect of hybrid molecules of terpenes and two synthetic anti-inflammatory agents in the ear edema model in mice [13]. However, the activity of these synthetic derivatives on key enzymes associated with the inflammatory response is unknown. The aim of the present work was to give an integrated interpretation of the biological activity data of the terpenyl esters of ibuprofen and naproxen by comparing the information obtained using animal experiments [13], enzyme inhibition assays against COX-2 and LOX and molecular docking studies.

2| METHODS AND MATERIALS

2.1. Synthesis

The starting compounds oleanolic acid, ferruginol and imbricatolic acid were isolated from natural sources as previously described [13]. The synthetic anti-inflammatory agents ibuprofen and naproxen were racemates from Laboratorio Chile with a purity > 95%. The synthesis of the ibuprofelyn and naproxenyl esters of the terpenes was carried out as previously reported [13].

2.2. *In vitro* inhibition of LOX

The inhibitory activity of the starting compounds (terpenes and synthetic anti-inflammatory drugs) and the hybrid molecules containing the terpene and the synthetic anti-inflammatory moieties against lipoxygenase (LOX) was carried out according to [14]. The assay is based on the enzymatic oxidation of linoleic acid to its hydroperoxide, which can be measured at 234 nm using a Unicam Spectronic (Genesys) spectrophotometer. The only commercially available LOX (Type I-B from *Glycine max*, Sigma L7395) was used for the experiments. Compounds were dissolved in DMSO and diluted to the final concentrations (50 µg/mL) using the reaction

buffer. The 100% activity controls were carried out using DMSO and buffer. The commercial NSAIDs ibuprofen and naproxen were used as reference compounds. All compounds were evaluated in triplicate and results are expressed as percent of inhibition ± *SD*.

2.3. *In vitro* inhibition of COX-2

The inhibition of COX-2 is based on the potential of the compounds to inhibit the conversion of arachidonic acid to prostaglandin H_2 (PGH_2) by human recombinant COX-2 [15]. The assay was carried out using a commercial kit (560131, Cayman Chemicals, Ann Arbor, MI, USA), following the supplier instructions. Compounds were dissolved in DMSO and diluted to the final concentrations (50 µg/mL) using the reaction buffer. The 100% activity controls were carried out using DMSO and buffer. $PGF_{2\alpha}$ produced from PGH_2 by chemical reduction with stannous chloride, was measured in a microplate reader (Biotek ELx 808) at 415 nm. The commercial NSAIDs ibuprofen and naproxen were used as reference compounds. All compounds were evaluated in triplicate and results are expressed as percent of inhibition ± *SD*.

2.4. Computational modeling studies

Molecular docking studies were carried out according to [16,17]. The computational method was used in order to suggest the possible binding modes and affinity of the compounds to human LOX and COX-2. The molecular docking calculations were carried out using 15-LOX isoenzyme considering previous reports on this enzyme and the dual inhibition studies with COX-2 [9,18]. This isoenzyme has a 42% degree of identity and 62% of similitude with 5-LOX. The alignment between the X-ray crystal structures of 5-LOX and 15-LOX is shown in supporting information (Supporting Figure 1), showing a RMSD value of only 1.68 Å.

The atomic coordinates for 15-LOX and COX-2 were obtained from the available X-ray crystal structures in Protein Data Bank (PDB) [19] with codes 4NRE and 4PH9, respectively. All X-ray crystal structures were prepared, refined and completed (when needed) using the *Protein Wizard Preparation* module available in Maestro visualization software [20]. All compounds were prepared using the software LigPrep [21], while the protonation states were predicted via the Epik program [22]. The analysis was performed using water as a solvent and pH 7.0. All obtained tautomers were further used in docking experiments.

Docking experiments were performed using Glide software in standard precision (SP) mode [23,24]. Glide docking uses a series of hierarchical filters to find the best possible ligand binding locations in a previously built receptor grid space. The filters include a systematic search approach, which samples the positional, conformational, and orientation space of the ligand before evaluating the energy interactions between the ligand and the protein. Grid boxes of 30 $Å^3$ and 32 $Å^3$ were first centered on the reference ligand co-crystallized with each targeted protein (ibuprofen in COX-2 and a substrate-mimic in 15-LOX) and default docking parameters were used. Those grid volumes assure an appropriate conformational sampling of compounds within the binding sites of studied enzymes and, thereby, a correct interpretation of relevant intermolecular interactions between compounds and enzyme residues. The docking poses for each ligand were analyzed by examining their relative total energy score. The more energetically favorable conformation was selected as the best pose.

2.5. Statistical analyses

The statistical analyses were carried out using the SPSS 14.0 software (IBM, Armonk, NY, USA). Statistically significant differences between samples were determined by one-way analysis of variance (ANOVA) followed by Tukey's multiple comparison test ($p = 0.05$).

3| RESULTS

3.1. Enzyme inhibition activity

The compounds (**6**-**15**) (Figure 1) were synthesized according to [13]. Compounds were tested at 50 µg/mL against COX-2 and LOX enzymes. The results are summarized in Table 1.

In the COX-2 assay, the activity of the starting diterpenes was significantly different for imbricatolic acid **2** compared to ferruginol **1** and oleanolic acid **3** (46.2, 29.5 and 32.8%, respectively). For the commercial NSAIDs, no significant difference was observed ($p < 0.05$). For the hybrid compounds using ferruginol as the terpene moiety (**6** and **7**), only the activity of the ferruginyl ibuprofenate (**6**) was significantly lower than the starting compounds. In the imbricatoyl derivatives (**8**-**11**), the compound imbricatol-15-yl naproxenate (**10**) showed an increase in the COX-2 inhibitory activity compared to the parent compound naproxen (**5**) ($p < 0.05$). Regarding the oleanolic acid derivatives (**12**-**15**), oleanoyl ibuprofenate (**12**) showed the highest inhibitory effect of the series, showing better activity than the parent compound oleanolic acid (**3**). In the ibuprofen derivatives, the activity was lower than that of the synthetic anti-inflammatory drug alone (57.3%). For the oleanoyl derivatives, the effect of the compound **12** was in the same range as ibuprofen but the effect decreased after methylation of

the COOH function in the triterpene. Interestingly, in the naproxen-oleanolic acid hybrids, the methyl ester group at C-28 increased the inhibition of COX-2.

In the LOX inhibitory assay, among the terpenes, only oleanolic acid (**3**) showed a marginal activity. For the commercial drugs, naproxen presented a 10 fold higher inhibitory effect compared to ibuprofen. In the hybrid compounds, all the naproxen derivatives (**7**, **10**, **11**, **14** and **15**) inhibited LOX in the range of 81.8-97.7%, which can be attributed to the naproxen moiety. Interestingly, oleanoyl ibuprofenate methyl ester (**13**) showed an increase in the inhibitory effect when compared to the parent compounds ibuprofen (**4**) and oleanolic acid (**3**).

3.2. Molecular Docking studies

The molecular docking conformations obtained for all inhibitors within the binding site of COX-2 and 15-LOX proteins are shown in Figure 2 and 3. Before the binding pose prediction of synthesized ligands against their protein targets, the docking protocol with Glide [23] was validated for each protein-ligand system by predicting the correct pose of X-ray co-crystallized ligand within reported protein binding site. In the case of COX-2, the predicted pose for ibuprofen was very close to its X-ray crystal structure, with a RMSD value of only 0.244 Å for heavy atoms. On the other hand, the best docked pose obtained for substrate mimic in 15-LOX deviates in 1.59 Å with respect to its structure in the X-ray crystal structure. Those initial docking results gave us confidence that the applied docking protocol with Glide [23] was capable to reproduce the X-ray crystal structure of co-crystalized ligands.

Figure 2A shows the docked structures of ligand **1** and its ibuprofen and naproxen hybrids **6** and **7**, respectively, within the COX-2 binding site.

As reference compounds we included: the co-crystallized structure of ibuprofen (represented in orange ball and sticks), the docked structures of ibuprofen (**4**, represented as yellow sticks) and naproxen (**5**, represented as spring green sticks). The carboxylate moiety of compounds **4** and **5** established a hydrogen bond (HB) interaction with residues Arg120 and Tyr355. The benzyl and naphthalene rings of these reference compounds are located in the hydrophobic pocket of COX-2 formed by residues Tyr385, Phe518, Val523 and Ser530 [8]. These interactions are in good agreement with the report of ibuprofen co-crystallized with COX-2 (PDB code: 4PH9) [4]. In the case of compound **1** and its hybrid compounds **6** and **7**, they are located within the COX-2 binding site. However, the compounds are not able to

establish the same HB interactions with residues Arg120 and Tyr355. Compound **1** is located in the same pocket as ibuprofen and naproxen but establishes only hydrophobic interactions with the residues at this site. Compounds **6** and **7** are located outside the pocket, establishing some π-stacking interactions with aromatic side chains of residues Tyr115 and Tyr355. The low percentages of *in vitro* inhibition shown by these compounds against COX-2 (22.2 and 32.2%, respectively) could be explained by: its relative big size to accommodate in the hydrophobic pocket, the lack of the carboxylate group (terpene **1**) and mostly by the hindered ester moiety that cannot establish HB interactions within the binding site (hybrids **6** and **7**).

Figure 2B depicts the docked poses for compounds **2**, **8 - 11** within the COX-2 binding site. The carboxylate moiety of terpene **2** forms two HBs with residue Arg120 and one additional HB with Tyr355, resembling those interactions formed by reference compounds **4** and **5**. The diterpene moiety is located in the same pocket as the reference compounds, establishing hydrophobic interactions with residues Tyr385, Phe518, Val523 and Ser530. Compounds **8**, **9**, **10** and **11** were able to establish HB interactions with residue Arg120 through the carbonyl group in the ester moiety that is less hindered that in compounds derived from terpene **1**. The benzyl and naphthalene rings in these compounds are located within the COX-2 binding in the same orientation that reference compounds **4** and **5**. An additional HB interaction is established by compounds **10** and **11** with residue Tyr355. The imbricatol moiety in all these derivatives is oriented towards the outer part of the binding pocket, probably establishing hydrophilic interactions with water. The improved inhibition percentages against COX-2 showed by these derivatives could be rationalized in terms of availability of their carbonyl ester to establish HB interactions with residues at COX-2 binding site. In addition, the ibuprofen and naproxen moieties of these hybrids show the same orientation as the reference compounds.

Figure 2C shows the best docking poses for compounds **3**, **12 - 15**. The size of these derivatives may suggest that they cannot fit within the COX-2 binding site. Instead, they could interfere with the enzyme function by blocking the entrance of the natural substrate to the binding pocket from different sides. No docking pose was obtained for compound **12**, thus suggesting that the high inhibition percentage against COX-2 (Table 1) may be achieved through another molecular mechanism like allosteric regulation or hindrance of the binding site entrance [25]. Compound **3**, **13** and **14** block the entrance to the main pocket of COX-2 in different extents. Compound **15** seems to block a second pocket that gives access to some ligands for the interaction with residues Arg513 and His90 [9]. A good correlation ($r^2 = 0.745$)

was obtained when comparing the COX-2 inhibition percentages and the relative docking energies calculated for compounds **1 - 15** (Table 2). The structural alignment between X-ray crystal structures for LOX-5 and LOX-15 and data plot for correlation between COX-2 percentage of inhibition and Glide docking score relative energy (kcal/mol) for studied compounds can be found in the Supporting Figure 1 and 2, respectively.

Figure 3 shows the docked structures of ligands **1-15** within the 15-LOX binding site. The binding site of 15-LOX is near the Fe^{3+} metal that is coordinated by residues Ile676, His373, His378 and His553 (Figure 3A). Two water molecules in the crystal structure complete the coordination sphere, but they were deleted in order to perform the docking calculations. Hydrophobic residues Leu420, Leu610, Ile412 and the solvent exposed residue Arg429, complete this binding pocket. The co-crystallized substrate-mimic (orange balls and sticks) fits in a U-shape form within the binding site, mostly establishing hydrophobic interactions with the above mentioned residues.

Docked structures of ibuprofen (**4**, yellow sticks) and naproxen (**5**, spring green sticks), are coordinating the iron atom through one of their oxygen carboxylate atoms (with distances about 2.2 Å). Their benzyl and naphthalene rings are located in the inner part of the pocket when compared with the substrate mimic.

Compounds **1**, **6** and **7** docked in the outermost and solvent exposed part of the binding pocket, establishing some hydrophobic interactions through their terpene rings. The ibuprofen and naproxen moieties of compounds **6** and **7** are oriented to the solvent. In addition, compound **6** establishes an HB interaction with residue Arg429.

4| DISCUSSION

4.1. Enzyme inhibition activity

When comparing the *in vitro* enzyme inhibitory activity of compounds **1-15** with that observed for the same derivatives in the topic anti-inflammatory model in the mice ear edema [13], several differences were found. The arachidonic acid (AA)-induced ear edema is associated with the inhibition of COX-1 and COX-2, while the phorbol 12-myristate 13-acetate (TPA)-induced topical inflammation is associated with LOX as main mechanism. In the *in vivo* experiments (expressed as percent inhibition compared with untreated controls), ferruginol **1** was active in both models, AA and TPA (21.0 and 20.4%, respectively). In the AA model, ibuprofen and

naproxen showed marginal activity (7.2 and 1.8%, respectively). However in the *in vitro* tests, compound **1** was less active than **4** and **5** in the COX-2 assay. Considering the hybrid compounds, it was reported [13], that compound **12** reduced by 56.8% the inflammation induced by AA. In the *in vitro* experiments, the same compound showed the highest inhibition activity against COX-2, while **10** and **15** were active against COX-2 but inactive in the *in vivo* experiments. The compound **12** was active both in the AA-induced ear edema and COX-2 *in vitro* inhibition.

When comparing the *in vivo* TPA model with the *in vitro* inhibition of LOX a similar effect was observed for the terpenes, being oleanolic acid (**3**) the most active in both assays (70.2 and 6.6%, respectively). On the contrary, naproxen (**5**) displayed low activity in the in vivo model, while the highest inhibitory effect in the *in vitro* studies (29.9 and 98.4%, respectively). In the *in vivo* experiments, terpenes and synthetic anti-inflammatory compounds were compared at the same equimolar dose. The compounds were applied topically at 1.4 and 3.2 µmol/mouse for 12-*O*-tetradecanoyl phorbol 13-acetate and the arachidonic acid assay, respectively [13]. Meanwhile, in the *in vitro* experiments the compounds were assayed at a single concentration of 50 µg/mL, which equates to 70-105 µM for the hybrid compounds.

A strong effect in the TPA-induced ear edema was observed for oleanoyl ibuprofenate (compound **12**, 79.9%), and oleanoyl naproxenate methyl ester (compound **15**, 80.0%), in the same range as the starting diterpene oleanolic acid (compound **3**, 70.2%) and higher than ibuprofen **4** (56.2%) [26]. However, in the *in vitro* LOX inhibition only compound **15** showed the same activity (Table 1).

In summary, when comparing the results in the *in vivo* models of inflammation and COX-2 inhibition, the most active compound was oleanoyl ibuprofenate **12** in both models; while for the *in vitro* LOX and TPA-induced edema in the mice ear, the best effect in both systems was for the oleanoyl naproxenate **14** and its methyl ester **15**.

4.2. Molecular Docking studies

Figure 3B shows the most probable docked poses for compounds **2**, **8** - **11** within 15-LOX binding site. Imbricatolic acid (**2**) binds at the entrance of the binding pocket forming two HBs with residues Arg429 and Ile420. Compounds **8**, **9**, **10** and **11** can bind in the same orientation that the co-crystalized substrate-mimic in a U-shape within 15-LOX binding site. Moreover, all

these compounds can coordinate the iron atom through their carbonyl groups at the ester moiety with distances between 2.77 to 3.18 Å. This finding could positively impact their capability to inhibit the enzyme when compared with those in ibuprofen or naproxen. However, the good fit of the naphthalene ring within the binding site and some HB interactions with residue Arg429 at the entrance of the pocket, could also be responsible for the good inhibitory activities shown by compounds **10** and **11**. For compounds **8** and **9**, despite that the benzyl rings also fit within the pocket, the orientation of the diterpene rings toward the solvent channel could negatively impact their desolvation entropic energy, thus penalizing their capability to effectively inhibit 15-LOX.

Figure 3C shows the most probably docking poses for compounds **3**, **12** - **15**. Oleanolic acid (**3**) cannot bind inside the 15-LOX binding site and, instead, it locates at the entrance of the pocket where it is mostly exposed to the solvent. On the other hand, compounds **12** and **13** also bind at the entrance of the 15-LOX binding pocket with their ibuprofen benzyl rings orientated to the iron atom, but incapable to form any stabilizing interaction with key residues at this site. This could explain their low and null inhibitory activities against this enzyme, respectively. Compounds **14** and **15**, bind at the entrance of the binding pocket, however, their stabilization is due to π-cation interactions between naproxen naphthalene rings and the charged residue Arg429. Compound **14** establishes an additional interaction with Arg429 through an HB which is mediated by a carbonyl group in its ester moiety. Those stabilizing non-covalent interactions could be responsible for their inhibitory activity against 15-LOX by blocking the binding pocket.

No significant correlation was found between docking energy (Table 2) and percentage of inhibition against 15-LOX. However, their inhibitory patterns could be explained by the structural interpretation of the conformations obtained with the molecular docking within the enzyme binding site. The binding site of 15-LOX seems to be flexible, as other macromolecular targets, and there is previous evidence that some induced fit docking protocols are needed in order to obtain good relationships between biological activity and docking energies, or most accurate, free binding energy methods for active ligands [26].

5| CONCLUSIONS

The synthesized hybrids showed an inhibition of COX-2 in the range of 9.8-57.4%. The LOX inhibition was in the range of 0-97.7%. None of the hybrids compounds showed an improvement in the inhibitory effect towards these pro-inflammatory enzymes, compared to the parent terpenes and commercial NSAIDs. However, the hybrids **7**, **11** and **15** showed strong inhibitory activity towards LOX and moderate inhibitory effect against COX-2. The molecular docking studies allowed us to predict the potential binding modes of hybrid molecules **1** - **15** within COX-2 and 15-LOX active sites. Moreover, the relative affinity of those compounds inside the binding sites could be explained in terms of their stabilization by forming non covalent interactions, like hydrogen bonds, π-stacking, π-cation and van der Waals, with most important and known amino acids reported for those proteins. A good correlation (r^2 =0.745) between molecular docking energies and percentage of inhibition showed by compounds against COX-2 enzyme was found. New synthetic possibilities could be obtained from our *in silico* models, aiming to improve the potency of this series of hybrid compounds.

ACKNOWLEDGEMENTS

We thank the financial support of FONDECYT (Projects 1110054 and 1130155) and PIEI-QUIM-BIO, Universidad de Talca. J.A-M. acknowledges Centro de Bioinformática y Simulación Molecular (CBSM) the access to computational time for performing molecular docking calculations.

CONFLICT OF INTEREST

The authors declare no conflict of interest.

FIGURE LEGENDS

FIGURE 1 Structure of the starting natural terpenes (**1-3**), synthetic anti-inflammatory drugs (**4-5**) and the ibuprofenyl and naproxenyl esters **6-15**.

FIGURE 2 Most probable conformations of compounds **1** - **15** within the COX-2 binding site. Protein carbon atoms are colored in gray and represented in balls and sticks. Non polar hydrogen atoms are not shown. Co-crystalized ibuprofen is represented as orange balls and sticks. Reference compounds **4** and **5** are represented as yellow and spring green sticks, respectively. Compounds **1**, **2** and **3** are represented in red thin sticks; compounds **6** and **8** are colored in blue; compounds **7**, **9** and **13** are colored in purple; compounds **8**, **10** and **14** are colored in dark green and compounds **9**, **11** and **15** are colored in plum. Hydrogen bond and π-stacking interactions are represented as yellow and cyan dashed lines, respectively. A) Docked poses of compounds **1**, **6**, **7**; B) Docked poses of compounds of compounds **2**, **8-11**; C) Docked poses for compounds **3**, **12-15**.

FIGURE 3 Most probable conformations of compounds **1** - **15** within 15-LOX binding site. Protein carbon atoms are colored in gray and represented in balls and sticks. Non polar hydrogen atoms are not shown. Co-crystalized substrate mimic is represented as orange balls and sticks and the iron atom is depicted in black. Reference compounds, **4** and **5**, are represented as yellow and spring green sticks, respectively. Compounds **1**, **2** and **3** are represented in red thin sticks; compounds **6**, **8** and **12** are colored in blue; compounds **7**, **9** and **13** are colored in purple; compounds **8**, **10** and **14** are colored in dark green and compounds **9**, **11** and **15** are colored in plum. Hydrogen bond and cation-π interactions are represented as yellow and green dashed lines, respectively. A) Docked poses of compounds **1**, **6**, **7**; B) Docked poses of compounds of compounds **2**, **8-11**; C) Docked poses for compounds **3**, **12-15**.

REFERENCES

[1] C.A. Rouzer, J. Lawrence, L.J. Marnett, *J. Lipid Res.* **2009**, *50*, S29–S34.

[2] L.J. Marnett, S.W. Rowlinson, D.C. Goodwin, A.S. Kalqutkar, C.A. Lanzo, *J. Biol. Chem.* **1999**, *274*, 22903-22906.

[3] N.V. Chandrasekharan, H. Dai, K.L. Roos, N.K. Evanson, J. Tomsik, T.S. Elton, D.L. Simmons, *Proc. Natl. Acad. Sci. USA* **2002**, *99*, 13926.

[4] A. Zarghi, S. Arfaei, *Iran J. Pharma. Res.* **2011**, *10*, 655.

[5] B.J. Orlando, M.J. Lucido, M.G. Malkowski, *J. Struct. Biol.* **2015**, *189*, 62.

[6] J.K. Gierse, J.J. McDonald, S.D. Hauser, S.H. Rangwala, C.M. Koboldt, K. Seibert, *J. Biol. Chem.* **1996**, *271*, 15810.

[7] A.R. Brash, *J. Biol. Chem.* **1999**, *274*, 23679.

[8] A. Rossi, C. Pergola, A. Koeberle, M. Hoffmann, F. Dhem, P. Bramanti, S. Cuzzocrea, O. Werz, L. Sautebin, *Brit. J. Pharmacol.* **2010**, *161*, 555.

[9] J. Kaur, A. Bhardwaj, Z. Huang, E.E. Knaus, *Chem. Med. Chem.* **2012**, *7*, 144.

[10] S. Ghatak, A. Vyas, S. Misra, P. O'Brien, A. Zambre, V.M. Fresco, R.R., Markwald, V. Swamy, Z. Afrasiabi, A. Choudhury, M., Khetmalas, S. Padhye, *Bioorg. Med. Chem. Lett.* **2014**, *24*, 317.

[11] R. Kodela, M. Chattopadhyay, K. Kashfi, *ACS Med. Chem. Lett.* **2012**, *3*, 257.

[12] A. Pawełczyk, D. Olender, K. Sowa-Kasprzak, L. Zaprutko, *Molecules*, **2016**, *21*, 420.

[13] C. Theoduloz, C. Delporte, G. Valenzuela-Barra, X. Silva, S. Cádiz, F. Bustamante, M.W. Pertino, G. Schmeda-Hirschmann, *Molecules*, **2015,** *20*, 11219.

[14] H. Wangensteen, A.B. Samuelsen, K.E. Malterud, *Food Chem.* **2004**, *88*, 293.

[15] M.S. Costamagna, I.C. Zampini, M.R. Alberto, S. Cuello, S. Torres, J. Perez, C. Quispe, G. Schmeda-Hirschmann, M.I. Isla, *Food Chem.* **2016**, *190*, 392.

[16] J.M. Blaney, J.S. Dixon, *Perspectives in Drug Discovery and Design 1*, **1993**, 301.

[17] D.B. Kitchen, H. Decornez, J.R. Furr, J. Bajorath, *Nat. Rev. Drug Discov.* **2004**, *3*, 935.

[18] C. Charlier, C. Michaux, *Eur. J. Med. Chem.*, **2003**, *38*, 645.

[19] H.M. Berman, J. Westbrook, Z. Feng, G. Gilliland, T.N. Bhat, H. Weissig, I.N. Shindyalov, P.E. Bourne, *Nucleic Acids Res.* **2000**, *28*, 235.

[20] Maestro, version 9.3, Schrödinger, LLC, New York, NY, **2012**.

[21] LigPrep, version 2.3, Schrödinger, LLC, New York, NY, **2009**.

[22] Epik, version 2.2, Schrödinger, LLC, New York, NY, **2011**.

[23] Glide, version 5.7, Schrödinger, LLC, New York, NY, **2011**.

[24] R.A. Friesner, J.L. Banks, R.B. Murphy, T.A. Halgren, J.J. Klicic, D.T. Mainz, M.P. Repasky, E.H. Knoll, M. Shelley, J.K. Perry, D.E. Shaw, P. Francis, P.S. Shenkin, *J. Med. Chem.* **2004**, *47*, 1739.

[25] M.M. Mitchener, D.J. Hermanson, E.M. Shockley, H.A. Brown, C.W. Lindsley, J. Reese, C.A. Rouzer, C.F. Lopez, L.J. Marnett, *PNAS* **2015**, *112***,** 12366-12371.

[26] J.B. Jameson, A. Kantz, L. Schultz, C. Kalyanaraman, M.P. Jacobson, D.J. Maloney, A. Jadhav, A. Simeonov, T.R. Holman, PLoS One **2014**, *11*, e104094.

SUPPORTING INFORMATION

Additional Supporting Information may be found online in the supporting information tab for this article.

TABLE 1 Percent inhibition of the terpenes (**1**-**3**), the synthetic anti-inflammatory drugs ibuprofen (**4**), naproxen (**5**) and the diterpenyl esters of ibuprofen and naproxen **6**-**15** on the enzymes COX-2 and LOX at 50 µg/ml.

Compounds	**COX-2 (%)**	**LOX (%)**
Ferruginol (**1**)	29. 5 ± 7.1[a]	Inactive
Imbricatolic acid (**2**)	46.2 ± 3.3[b,h,i]	Inactive
Oleanolic acid (**3**)	32.8 ± 2.5[a,c,d]	6.60 ± 0.6[a]
Ibuprofen (**4**)	57.3 ± 6.0[b,h,i]	9.8 ± 0.6[a]
Naproxen (**5**)	44.2 ± 4.1[b,d,f]	98.4 ± 2.1[b]
Ferruginyl ibuprofenate (**6**)	22.2 ± 1.9[a,e,f]	10.6 ± 1.7[a]
Ferruginyl naproxenate (**7**)	32.2 ± 3.0[a,d,f]	95.0 ± 7.1[b,c]
Imbricatol-15-yl ibuprofenate (**8**)	9. 8 ± 0.8[g]	Inactive
Imbricatol-15-yl ibuprofenate methyl ester (**9**)	44.8 ± 3.8[b,c,i]	Inactive
Imbricatol-15-yl naproxenate (**10**)	57.4 ± 5.1[h,i]	81.8 ± 4.4[d]
Imbricatol-15-yl naproxenate methyl ester (**11**)	40.6 ± 3.5[a,b,c]	97.7 ± 3.3[b]
Oleanoyl ibuprofenate (**12**)	56.3 ± 5.1[b,h,i]	Inactive
Oleanoyl ibuprofenate methyl ester (**13**)	29.6 ± 2.7[a,c]	21.9 ± 3.5[e]
Oleanoyl naproxenate (**14**)	14.5 ± 1.3[e,g]	87.4 ± 2.8[c,d]
Oleanoyl naproxenate methyl ester (**15**)	45. 6 ± 4.4[b,h,i]	86.3 ± 3.9[c,d]

[(a-i)] Different letters in the same column show significant differences within each compound, according to Tukey's test ($p < 0.05$).

TABLE 2 Glide docking score energies for the studied compounds against COX-2 and 15-LOX

Compound	COX-2 Glide SP Emodel (kcal/mol)	15-LOX Glide SP Emodel (kcal/mol)
1	-23.60	-35,09
2	-52.67	-45,20
3	-15.97	-48,08
4	-65.46	-63,87
5	-76.57	-68,91
6	-16.89	-44,49
7	-4.52	-35,08
8	-56.52	-93,91
9	-53.77	-93,50
10	-79.89	-90,25
11	-59.91	-98,40
12	n/d	-61,87
13	-25.37	-55,59
14	-32.90	-63,05
15	-53.13	-42,95

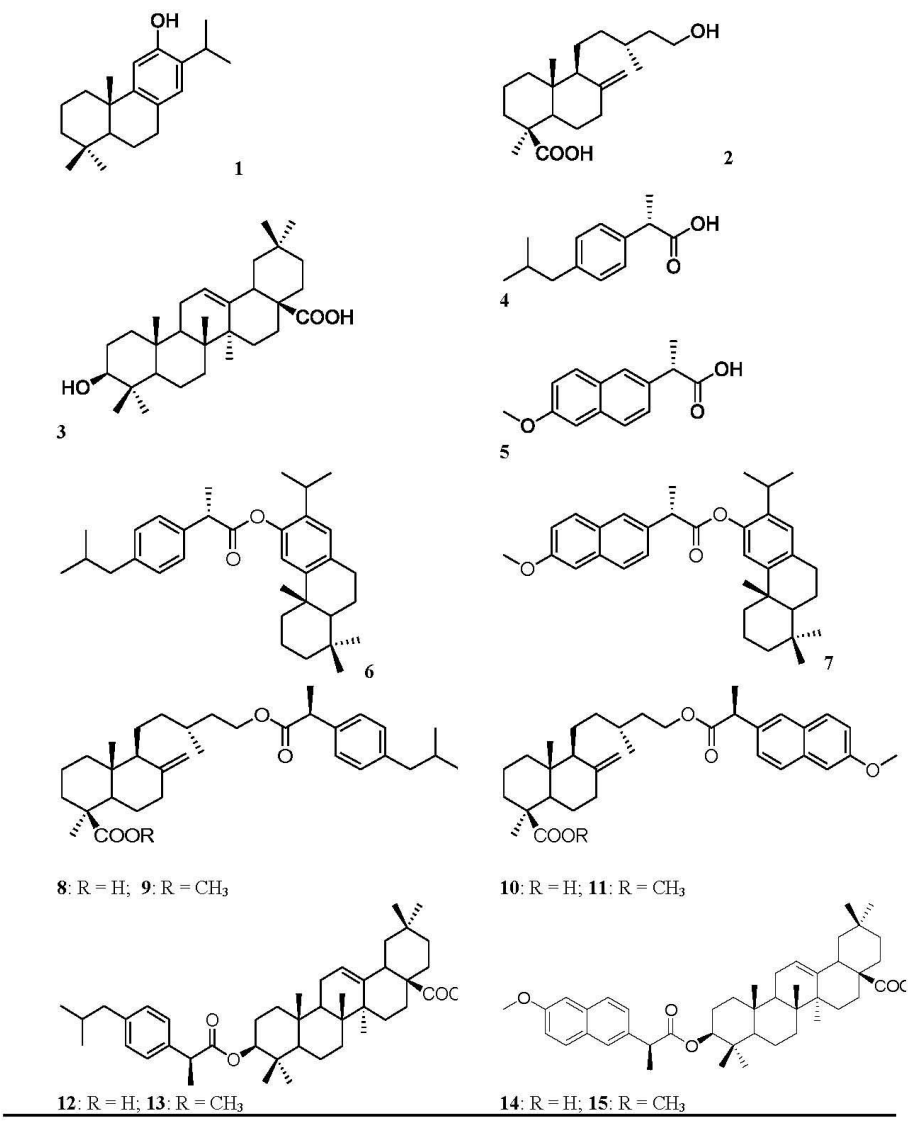

Figure 1.

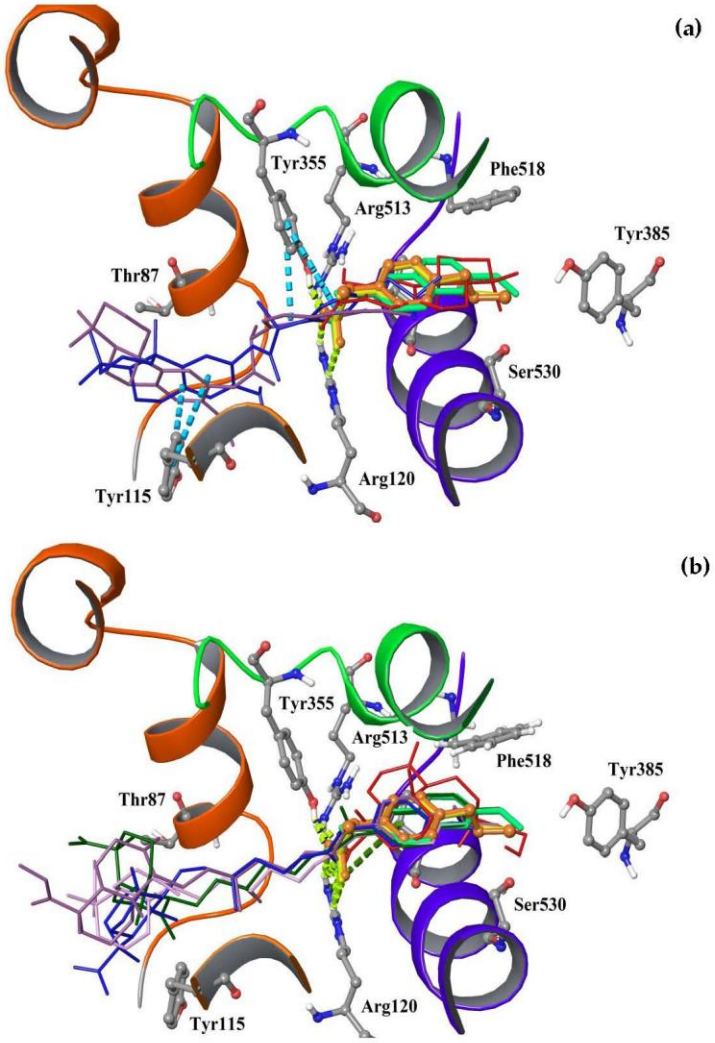

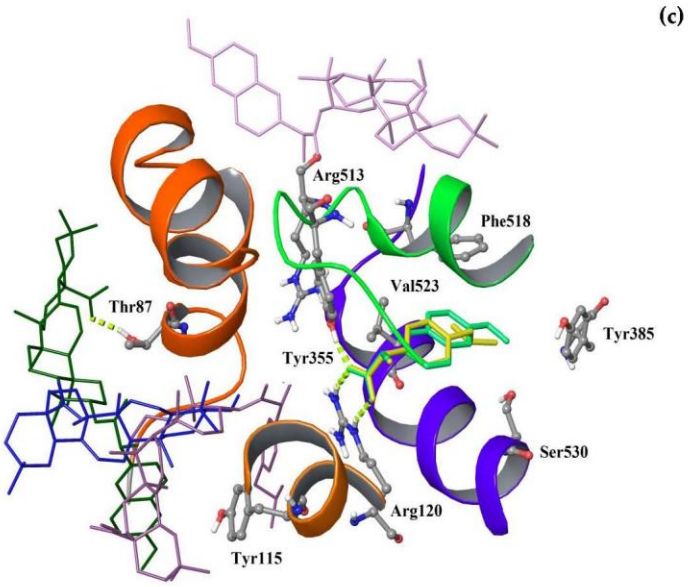

Figure 2

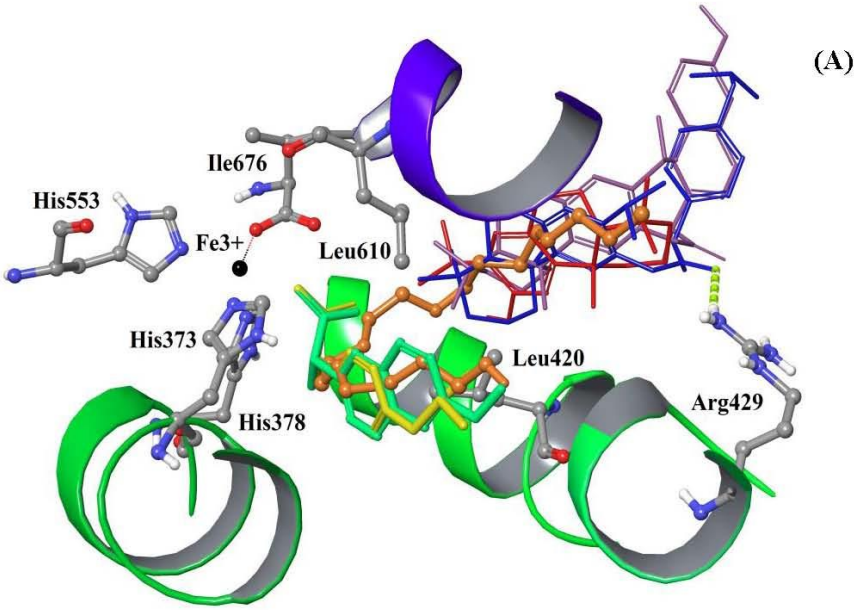

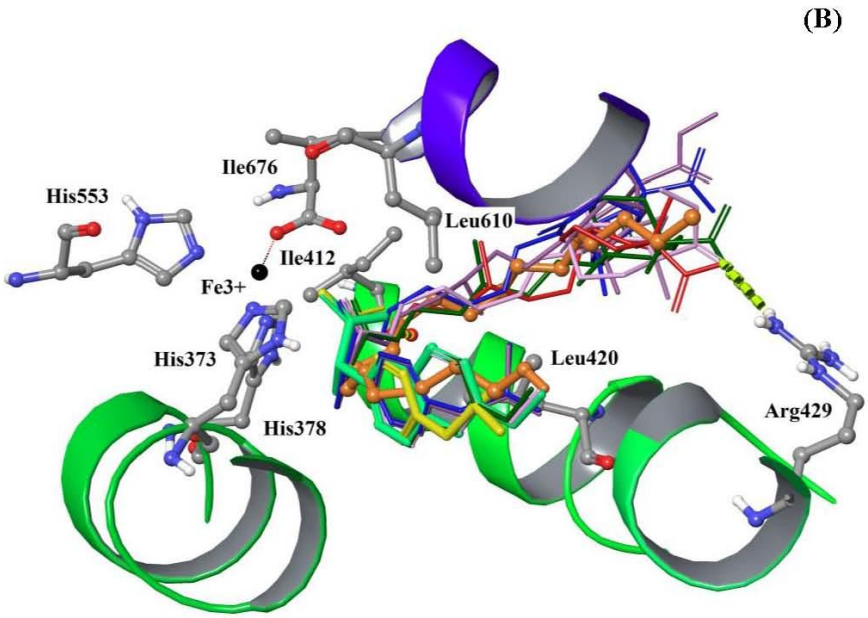

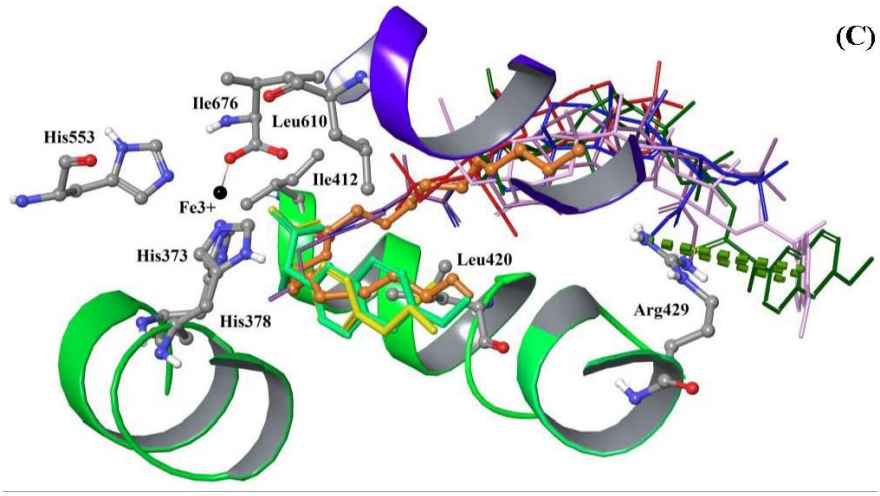

Figure 3